Published in final edited form as:
Biochim Biophys Acta. 2010 April ; 1798(4): 788–800. doi:10.1016/j.bbamem.2009.11.024.

Infrared Reflection-Absorption Spectroscopy: Principles and Applications to Lipid-Protein Interaction in Langmuir Films

Richard Mendelsohn, **Guangru Mao**, and **Carol R. Flach**
Department of Chemistry, Newark College, Rutgers University, 73 Warren Street, Newark, New Jersey, USA, 07102

Abstract

Infrared reflection-absorption spectroscopy (IRRAS) of lipid/protein monolayer films *in situ* at the air/water interface provides unique molecular structure and orientation information from the film constituents. The technique is thus well suited for studies of lipid/protein interaction in a physiologically relevant environment. Initially, the nature of the IRRAS experiment is described and the molecular structure information that may be obtained is recapitulated. Subsequently, several types of applications, including the determination of lipid chain conformation and tilt as well as elucidation of protein secondary structure are reviewed. The current article attempts to provide the reader with an understanding of the current capabilities of IRRAS instrumentation and the type of results that have been achieved to date from IRRAS studies of lipids, proteins and lipid/protein films of progressively increasing complexity. Finally, possible extensions of the technology are briefly considered.

A. Background

(1) Monolayers as a paradigm for studies of lipid–protein interaction

The study of lipid-protein interaction in model membrane systems has been approached by a wide variety of biophysical methods, as amply demonstrated in this volume. Such investigations have been greatly aided in the past two decades by technical advances, including methods for acquisition of 3D structures of membrane proteins and by refinements in molecular modeling of bilayer systems. Despite substantial progress, certain classes of problems are not adequately addressed with bilayers as the sole experimental paradigm. For example, an understanding of the initial recognition events between proteins and membrane surfaces may require a degree of control of the physical properties of the interface not always available in bilayer or multilayer systems.

The advantages of lipid monolayers as experimental models for biophysical studies have been well recognized. An example of a problem of physiological relevance which benefits from monolayer studies is the mechanism of pulmonary surfactant action. Accordingly, lipid-protein films at the air-alveolar lining layer in the mammalian lung are thought to exist *in vivo* as pressure-dependent monolayers and multilayers [1,2]. Another specific class of problem for which monolayers are appropriate involves interfacial enzymes such as the phospholipases. Thus, phospholipase A_2 is 10^4 times more active with phospholipid substrates organized as

monolayers rather than in their monomeric states [3]. More generally, any interacting lipid-protein pair for which the initial recognition steps are of interest may be profitably studied by monolayer-based approaches.

From an experimental viewpoint, lipid monolayers at the air/water interface (Langmuir films) as models for studies of lipid-protein interaction provide several technical advantages. First, aqueous substrates are obviously the most relevant biologically, especially when compared to solid surfaces. Second, from a biophysical point of view, many useful experimental variables may be controlled, including surface pressure, monolayer and subphase composition (including the presence of proteins), area/molecule, temperature, pH, and phase separation/domain formation in lipid mixtures. The study of monolayers also offers the practical advantage of requiring small amounts (micrograms) of occasionally expensive protein constructs (e.g. genetically engineered) compared with bulk phase measurements. A drawback to the use of Langmuir films as an experimental paradigm prior to the mid 1980's was that molecular structure information could not be acquired from film constituents. Information was more or less limited to the classical techniques of pressure-area (π-A) isotherms.

The situation changed significantly in the mid 1980's. Techniques such as (epi-) fluorescence microscopy, Brewster angle microscopy, and X-ray reflection, became available for studies of the organization of Langmuir films [4-7]. Although these approaches provide no direct molecular structure information, they provide essential characterization of film organization and phase behavior at supramolecular distance scales. At high pressures such as those occurring in relevant lung models (solid or liquid–condensed phases), the contrast in fluorescence or Brewster angle microscopy imaging experiments becomes limited.

A difficulty in acquiring molecular structure information from film constituents arises in that the standard high resolution tools of biophysics, e.g. NMR or X-ray diffraction, are not applicable. Thus, the experiments of Dluhy and his associates [8-11] from the mid 1980's showing that it was possible to acquire molecular structure information from lipid monolayers *in situ* at the A/W interface using IR spectroscopy, were very welcome. The technique they employed was a variant of IR termed infrared reflection-absorption spectroscopy (IRRAS). Following initial reports that monitored acyl chain structural changes during surface pressure-induced phase transitions, applications of IRRAS were expanded both by this laboratory and others to monitor elements of lipid and protein structure and orientation [12-17]. The theory and applications have been reviewed several times [18-22]. Since the subject matter is generally unfamiliar, the technique is summarized briefly below for the reader's convenience.

(2) IRRAS-Experimental Considerations

IRRAS is based on the observation that when mid-IR radiation impinges onto aqueous monolayers films, a small fraction (6%) of the light is reflected from the molecular constituents of the surface. IRRAS spectra of the film constituents are generally presented as plots of reflectance-absorbance (RA) *vs* wavenumber. RA is defined as $-\log_{10}(R/R_o)$ where R is the reflectivity of the film-covered surface and R_o is the reflectivity of the aqueous subphase.

A schematic of the experimental set-up currently in use at Rutgers University is shown in Figure 1. Light in a well-defined polarization state, either parallel (p-polarized) or perpendicular (s-polarized) to the plane of incidence, impinges onto the surface at a well defined and controlled angle of incidence. The reflected light is detected at an angle equal to the angle of incidence. The polarization state of the beam and the surface pressure of the Langmuir film are computer controlled and adjusted as desired. Lipid films are generally spread from volatile organic solvents. Proteins may be spread concurrently with or without lipids directly on the surface or, alternatively, injected directly into the subphase beneath the surface and their subsequent adsorption to the monolayer measured.

A major impediment to the acquisition of good quality IRRAS spectra from films on aqueous surfaces is the spectral interference from the omnipresent rotation-vibration bands from water vapor. To overcome this problem, two approaches have been developed. The Rutgers group developed [23] a sample shuttle technique in which a reference IRRAS spectrum is acquired from a film-free surface. The intensity of light reflected from the film-covered surface is then ratioed to the reference spectrum. Residual interference from water vapor and other sources of noise are reduced to ~2×10^{-5} RA units. To overcome spectral interference in the Amide I region from the H_2O bending mode, D_2O is often used in the subphase. A typical example from the Rutgers lab is shown for a 4-component (DPPC/DPPG/Cholesterol/SP-C) model of pulmonary surfactant in Figure 2. The S/N ratio in the C-H stretching region is 300/1 for the 2850 cm^{-1} symmetric stretching mode (RA ~ .003) and the Amide I mode of SP-C near 1650 cm^{-1} is readily detected.

An alternative approach, termed polarization modulation-infrared reflection-adsorption spectroscopy (PM-IRRAS), developed primarily by the Bordeaux group [15,24], possesses an advantage over the conventional IRRAS mode in that the modulated reflectivity is independent of the isotropic adsorption from vapor or bulk water. In this experiment, a photoelastic modulator generates alternating linear states of polarized light. Consequently the interfering effect of water vapor and carbon dioxide can be substantially reduced.

(3) Analysis of IRRAS spectra

(i) Interpretation of IR frequency information—As in most IR experiments, IRRAS measurements provide frequencies and intensities of molecular vibrations. There are several levels of sophistication at which spectral frequencies from relatively large molecules may be interpreted. In general, for lipids, peptides, and proteins, the normal coordinate problem is underdetermined, even with extensive use of isotope labels. Empirical levels of analysis, developed over the past half-century, are routinely applied. These assume that spectra-structure correlations established for small molecules may be directly transferred to lipid assemblies or proteins. The added notion that must be considered for useful extrapolation of spectra-structure correlations from small molecules to polymers is the occurrence of vibrational coupling between identical or nearly identical chemical units. Snyder (US)[25,26], Zerbi (Italy)[27] and Shimanouchi (Japan)[28,29] have extensively developed these concepts for molecules containing polymethylene chains. Many groups, including ours, have attempted to calculate the effects of vibrational coupling on the IR and Raman spectra of proteins in solution. We have expounded this work in detail for antiparallel ß-sheets[30], for model collagen peptides [31] and for globular proteins[32]. Spectral features usually available from IRRAS measurements and the sensitivity of particular vibrational modes to molecular structure changes are summarized in Table 1.

(ii) Interpretation of IRRAS intensities—Whereas IRRAS frequency information is interpreted in terms of molecular structure as noted above, a detailed examination of IRRAS intensities permits determination of the orientation of functional groups or ordered structural elements (lipid chains, protein helices or sheets, etc.) and requires consideration of the optical properties of the interface. Reflected intensities at frequencies corresponding to molecular vibrations depend upon extinction coefficients, the experimental geometry (angle of incidence, state of polarization of the radiation), the optical constants (real and imaginary parts of the refractive indices of the film and subphase), and the orientation of the vibrational transition moments relative to the incident plane of illumination. In normal IR, absorbance is a positive quantity. In contrast, RA's may be positive or negative, depending on the parameters noted above.

Our summary of the various theories of IRRAS intensities was published some 15 years ago [21], and the approaches seem to have stood the test of time. Several groups have found that the treatment of Kuzmin, Michailov, and co-workers[33-35] that assumes a framework based on a thin anisotropic Langmuir film between two semi-infinite phases (air, water) gives reflected IRRAS intensities in good agreement with experiment. The interested reader is thus referred to the above sources.

(4) Sensitivity and reproducibility of IRRAS measurements

The current state of IRRAS reproducibility with the apparatus shown in Figure 1 is demonstrated below and in Flach et al., 2001[36]. Figures 3A,B show both p- and s-polarized IRRAS spectra of the methylene stretching modes for a skin lipid (ceramide 2, structure given in the Figure) at a series of angles of incidence between 40 and 70°. Spectra are offset for clarity. In Figure 3A, where spectra acquired with p-polarized light are plotted, two features are of interest. The sign change of the RA at the Brewster angle is predicted by the theory, while the subtle difference in the response of the two methylene stretching modes at 2850 and 2920 cm^{-1} to changes in the angle of incidence arises from slight differences in the subphase optical constants at the two frequencies. Figure 3 C and D show the reproducibility of the data for 4 independent preparations for both p- and s- polarizations.

The instrument precision demonstrated in Figure 3 is translated into increased precision in orientation measurements. The benefits accrued are demonstrated for an experiment where IRRAS was used [37] in an attempt to verify the assumed orientation of the C=O bond in behenic acid methyl ester (structure shown in Figure 4) monolayers at the A/W interface. IR spectra of BME shows two strong C=O bands at 1737 and 1721 cm^{-1} arising from unhydrated and hydrated C=O bonds respectively, as well as weaker features not considered here. IRRAS spectra are shown in Figures 4A, B for the two polarizations at various angles of incidence.

Elementary bonding considerations suggest that the unhydrated C=O is perpendicular to the BME chain which itself is known [38,39] to be perpendicular to the surface. The system thus serves as a sensitive test of the formalism for calculating the orientation of particular functional groups. The predicted 90° angle of the C=O bond relative to the chain is borne out by the IRRAS measurements. The intensity ratio of P/S polarized spectra of the 1737 cm^{-1} band is compared in Figure 4C with the theoretical simulations presented as a solid line in the figure, assuming the aforementioned 90° angle. The excellent agreement indicates (i) that the experimental measurements are precise enough to determine functional group orientation and (ii) that the simulation methods are appropriate. It is noted that it is very difficult to acquire IRRAS spectra with good S/N ratios utilizing P-polarized radiation at incident angles between 48-58°, i.e. close to the Brewster angle, due to the weakness of the reflected intensity. Spectra at angles of incidence greater than 60° are easier to acquire.

B. Applications of IRRAS for Structural Studies of Lipid and Proteins

The purpose of the current chapter is to demonstrate the scope of applications possible with current IRRAS technology, rather than to comprehensively review the literature. As noted above, several reviews spanning the past 2 decades of applications are readily accessible. The experiments selected herein include examples of i) lipid monolayers-molecular structure and phase behavior, ii) peptide monolayers - secondary structure, and orientation, iii) lipid/peptide and lipid/protein interactions, iv) lipid -protein interactions in phospholipase-catalyzed hydrolysis of PC’s, and lastly, v) a recent application involving the pulmonary surfactant system.

(1) Lipid monolayers - molecular structure and phase behavior

Initial applications of IRRAS centered on characterization of chain conformational changes in Langmuir monolayer films. An early example from Dluhy's group [18,40] is shown in Figure 5. The CH_2 stretching region from a series of IRRAS spectra acquired from a DPPC monolayer at progressively increasing surface areas are overlaid (from lower to higher (negative) peak intensities). These vibrational frequencies are well-known to decrease with the introduction of conformational order into the acyl chains. Thus, the decrease in the asymmetric CH_2 stretching frequency from ~ 2922.5 to ~ 2917 cm^{-1} as the DPPC monolayer is compressed through various phases with decreasing area/molecule provides unique information about gauche rotamer formation in each physical state of the monolayer.

In addition to qualitative information about chain conformation, the theoretical formalism may be used to acquire precise information about chain tilt angles in ordered phases. An example from the laboratory of Professor Arne Gericke (Kent State University) is shown in Figure 6. Measured and calculated RA values as a function of angle of incidence for the symmetric CD_2 stretching vibration are plotted for a monolayer of acyl chain perdeuterated DPPC (DPPC-d_{62}) on an H_2O subphase at a surface pressure of 28 mN/m. The best fit to the experimental data as shown was found for an acyl chain tilt angle of 26°. The calculated curves and experimental data points are shown for s- and p- polarization. Excellent agreement is evident.

IRRAS measurements also provide insight about events in the polar regions of the monolayer films. An example is shown for the phosphate groups of diphosphoryl Lipid A, a precursor of lipopolysaccharide (LPS) whose structure is shown in Figure 7A. The 1190-1300 cm^{-1} region is plotted as a function of surface pressure in Figure 7B. This spectral region contains the asymmetric PO_2^- symmetric stretching vibration, a mode that is very sensitive to phosphate group hydration (i.e. H-bond formation). At the lowest surface pressures, the band contour consists of (at least) three overlapped features at ~1225, 1238 and 1258 cm^{-1}, probably corresponding to dihydrated, monohydrated, and unhydrated phosphate groups respectively. As the surface pressure is increased, it is evident that IR intensity is transferred from the dihydrated to the monohydrated form. The simplest interpretation of this experiment is that it reveals a structural or environmental change in the vicinity of one of the lipid polar head groups resulting in a change in accessibility of water to the phosphates. It is interesting to observe that one of the phosphates remains dehydrated throughout the isotherm, as evidenced by the nearly constant relative intensity of the peak at 1258 cm^{-1}.

In a final demonstration of the unique capabilities of IRRAS, Desbat and collaborators [41] have utilized a Langmuir trough design (Figure 8A) which permits acquisition of data at high surface pressure. In the normal IRRAS set-up, the flat barrier lies directly on the edge of the trough as shown in the top panel. The modified barrier shown in the bottom panel is embedded in the trough and allows the water level to be adjusted. This design prevents rupture of the liquid meniscus at high surface pressures. PM-IRRAS and Brewster Angle Microscopy data acquired from monolayers compressed in this trough beyond the point of collapse have shown the formation of stable multilayer structures. For example, as shown in Figure 8B, compression of 1,2-dioleoyl-phosphatidylserine (DOPS), to pressures greater than ~45 mN/m, revealed the presence of a trilayer structure. As shown in the Figure, IRRAS intensities of the methylene modes and the lipid C=O are ~ 3× greater than those from the monolayer. Similar conclusions are evident from the low frequency region shown in the bottom panel.

(2) Peptide monolayers - secondary structure, and orientation

IRRAS provides a unique means to study protein conformation in monolayer films. Three examples are given below that emphasize current IRRAS capabilities in this area. The first experiment monitors long term temporal stability of protein structure in films alone and in the

presence of lipids at the interface. The protein used was a genetically engineered construct of pulmonary surfactant protein SP-A, a molecule involved in innate host defense against airborne pathogens. The current variant includes the carbohydrate recognition (CRD) and neck regions of the molecule. The protein adsorbs directly to aqueous surfaces, in this case D_2O, and the temporal variation of the Amide I' contour is shown in Figure 9A. The Amide I' region initially reflects the known mixed helical and irregular structure of the construct. Spectral shifts consistent with the formation of substantial proportions of β strands or sheets become evident after ~5 hours, the result of surface denaturation. The unfolding is inhibited by the presence of a Lipid A film. In this case, shown in Figure 9B, no significant change in SP-A structure was observed for 6.5 hr. Similar types of experiments have been reported by Lad et al., who studied the interaction of lysozyme with stearic acid monolayers [42].

The second application to protein films involves the monitoring and localization of surface–pressure induced secondary structure changes in the peptide fragment 9-36 of the pulmonary surfactant protein SP-B [43]. The peptide sequence is NH_2-WLARALIKRIAQMIPKGA*LA*VA*VA*Q-VCR-COOH. Two isotopomers of the peptide were synthesized, the normal isotopic form, as well as the form possessing ^{13}C peptide bond C=O groups in the four alanine residues indicated by asterisks in the sequence. The full length protein possesses a four helix bundle motif. The Amide I' IRRAS spectral region (1750-1540 cm^{-1}) from native, porcine SP-B, and from the labeled and unlabeled SP-B:9-36 peptide monolayers are shown in Figure 10. The native full length protein shows a mixed helical and disordered secondary conformation, while the unlabeled peptide shows an additional spectral feature at ~1624 cm^{-1}, revealing the presence of β structure. The labeling experiment permits the conclusion that the residues involved in the β structure arise from the labeled region of the peptide. The shift from 1624 cm^{-1} (unlabeled molecule) to 1597 cm^{-1} (labeled molecule) without substantial additional changes in the Amide I' contour, provides firm evidence for this assignment. The "take-home" message from this experiment is that IRRAS technology now has sufficient sensitivity to identify those regions of peptides and small proteins undergoing conformational alterations.

A third extremely useful application of IRRAS for examination of peptide monolayers is the determination of peptide orientation. For complex systems, independent knowledge of the peptide structure is required. Losche, Blume, and their associates [44] examined monolayers of Neuropeptide Y (NPY), a 36 amino acid neurotransmitter with sequence YPSKPDNPGEDAPAEDMARYYSALRHYINLITRQRY-NH_2 and an amidated C-terminus. It is found throughout the central and peripheral nervous system in many mammalian species. NMR data in solution [45] reveals the presence of an amphiphilic α-helix, spanning residues 13- 36, while the N-terminal part of the peptide is disordered.

The approach used to derive peptide orientation is summarized in Figure 11. The primary spectral data depict the Amide I region from a pure peptide film at the four surface pressures marked on the isotherm in the top half of Figure 11A. Spectra were acquired with p-polarized radiation at angles of incidence of 40° and 60°. Included with the isotherm is a helical wheel structural representation.

IRRAS spectra simulated according to the theoretical formalism of Kuzmin and Michailov are shown in Figure 11B. When the amphipathic helix is assumed to lie parallel to the interface (φ =90° in the simulation), a purely negative contour is predicted for the Amide I mode for an angle of incidence of 40°, while a purely positive contour is predicted for the Amide I mode for an angle of incidence of 60°. Comparison of simulation with experiment reveals that the peptide orientation is essentially parallel to the interface. It is noted the observed shift of ~ 8 cm^{-1} in Amide I frequency between the spectra acquired at 40° and 60° angle of incidence is accounted for in the simulations.

(3) Lipid/peptide and lipid/protein interactions

As is clear (hopefully) at this point, IRRAS is particularly well suited for the study of lipid/protein interaction. The obvious reason for this is that the experiment provides otherwise unobtainable information about the lipid and protein constituents of the monolayer. Two examples of the effect of protein on the tilt of the acyl chains in mixed lipid-protein monolayers are presented. In the first example (Figure 12), IRRAS was used to monitor the interaction of pulmonary surfactant SP-A with preformed DPPC monolayers as a function of surface pressure [46]. Typical experimental data points for the RA of the symmetric CH_2 stretching vibration of DPPC are shown in Figure 12 for two surface pressures and for two polarizations in the presence and absence of protein.

Incorporation of SP-A at surface pressures of 10 mN/m induces a significant decrease in the average acyl chain tilt from 35° to 28°. In contrast, little or no protein-induced change in DPPC chain tilt was observed at surface pressures of 25 or 40 mN/m (data not shown for a pressure of 40 mN/m). These results are consistent with fluorescence microscopy studies[47] in which SP-A was suggested to accumulate at the boundary between LE and LC domains. Thus the lack of change in DPPC chain tilt at high pressure suggests that the protein is excluded from the very ordered lipidic environment.

In an elegant early PM-IRRAS study of the effect of lipid on protein conformation, Ulrich and Vogel examined monolayers of gramicidin A, pure and in mixtures with dimyristoylphosphatidylcholine (DMPC), at the air/H_2O and air/D_2O interfaces by (PM-IRRAS)[16]. The entire set of amide I absorption modes were simulated for various possible structures of the protein, using complete parameter sets for different conformations based on published normal mode calculations. The structure of gramicidin A in the monolayer was assigned to a 6.3 helix. PM-IRRAS spectra of a DMPC/gramicidin A mixed monolayer on a D_2O subphase at different surface pressures are shown in Figure 13A, while simulated PM-IRRAS spectra at various gramicidin A tilt angles are shown in Figure 13B. Excellent agreement between the simulated and experimentally observed Amide I contours is noted. A marked dependence of the peptide orientation on the applied surface pressure was observed for the mixed lipid-peptide monolayers. At low pressures the helix lies flat on the surface, whereas at high pressures the helix was oriented almost parallel to the surface normal.

(4) Lipid -protein interactions in phospholipase- catalyzed hydrolysis of PC's

As noted in the Introduction, the physical state of phospholipid substrates for phospholipase action dramatically effects the rate of hydrolysis. IRRAS provides a convenient means to probe this phenomenon. The Möhwald/Brezesinski group has provided interesting results in this area [48-50]. A useful example from their lab shown in Figure 14 is their IRRAS examination of the phospholipase D catalyzed hydrolysis of DPPC to produce 1,2-dipalmitoylphosphatidic acid (DPPA) [48]. They took advantage of spectral differences between DPPA and DPPC in the spectral region (1000-1270 cm^{-1}) of the PO_2^- stretching modes to develop an assay for the extent of hydrolysis of DPPC catalyzed by phospholipase D. Spectra providing the basis for the assay are shown in Figure 14 A in which PM-IRRAS spectra of DPPA/DPPC mixture are plotted as a function of composition, while Figure 14B plots the integrated intensity of various phosphate vibrations arising from either DPPA or DPPC as a function of the mole fraction of DPPC. This straightforward calibration permits determination of the extent of DPPC hydrolysis at two enzyme concentrations as shown in Figure 14C.

(5) Lipid –Protein Interaction in the pulmonary surfactant system

Two recent examples from this laboratory [51], describing applications of IRRAS for studies related to the pulmonary system, are presented. For a more thorough sampling of recent

applications of IRRAS to studies of pulmonary surfactant, the reader is referred to the following original literature [52-54].

i) Ca^{2+} -induced binding of SP-D nCRD to LPS—Two of the pulmonary surfactant specific proteins, SP-A and SP-D, are known to play a role in host defense. The roles played have been described in general terms; however, the molecular mechanisms of the specific recognition between these proteins and lectins are not yet fully elucidated. It is known that SP-D binds the core carbohydrate region of various lipopolysachharides (LPS) found in Gram-negative bacteria cell walls. As a starting point for understanding the molecular basis of binding, useful structural information has been acquired from recombinant trimeric fragments of human and rat SP-D [55-57].

We undertook IRRAS studies [51] of SP-D/LPS interaction since structural information regarding SP-D binding to physiologically relevant ligands was unavailable. Two types of experiments were undertaken. First, IRRAS was used to qualitatively monitor the binding of SP-D to an LPS molecule. Typical experimental data are shown in Figure 15.

IRRAS spectra (1765-1540 cm^{-1}) are shown for the Ca^{2+}-specific binding of recombinant trimeric SP-D, possessing the neck and carbohydrate recognition domain (NCRD), to Rd_1 LPS monolayers. Monolayers were initially compressed to surface pressures of 10 mN/m (Figure 15A) or 25 mN/m (Figure 15B). Spectra were acquired prior to and following protein injection and pressure equilibration as indicated (steps 1,2 in each panel). Subsequently, an EDTA solution was injected into the subphase, and spectra were acquired after 10 min and 1 h (steps 3 and 4 in each panel). The Ca^{2+}-dependent nature of LPS binding was proven by this protocol since spectra acquired at different times after the addition of EDTA display a significant decrease in SP-D Amide I intensity with time indicating its release from the surface. As seen in the spectra, after approximately 1hr, a moderate surface pressure increase was observed along with an additional IRRAS shoulder at ~1615 cm^{-1}, most likely due to the carboxylate asymmetric stretch of EDTA.

(ii) Orientation of SP-D in a lipopolysaccharide film—In addition to the qualitative demonstration of Ca^{2+}-dependent binding outlined above, a quantitative determination of the orientation of the SP-D NCRD to the LPS monolayer was carried out. The analysis involved detailed simulations of the Amide I contour using procedures developed in the Rutgers lab [32], followed by incorporation of the Kuzmin/Michailov formalism to calculate the IRRAS intensities. The results are shown in Figure 16. In the Figure, the experimental dichroic ratio (p-polarized intensity/s-polarized intensity) values at 1654 cm^{-1} (most sensitive frequency for determining the neck orientation-see [51]) measured using three different sets of conditions are plotted over a range of incident angles along with curves generated from simulated intensities calculated for various assumed tilt angles as indicated. The experimental values were obtained from SP-D NCRD adsorption to a clean A/W interface and to LPS (Rd_1) monolayers at surface pressures of 10 and 25 mN/m. The simulated curves are based on the X-ray structure coordinates of the L,D-heptose-bound protein structure [55]. The best fit to the experimental data in the absence of an LPS monolayer was found for the simulations where the molecular axis was essentially parallel to the A/W interface, i.e., a tilt angle close to 90°. In contrast, in the presence of LPS monolayers, a best fit tilt angle range of 20-45° was found for the π = 10 mN/m experiment whereas a tilt angle closer to 20° fit the data for the LPS π = 25 mN/m experiment.

(C) Future prospects

Two decades following its introduction, IRRAS is well-integrated into the standard set of tools for evaluation of molecular structure in Langmuir films. Several areas of biophysics, as noted

above, have benefitted significantly from this technology. Future progress in the field awaits technical improvements currently on the horizon. For example, incorporation of spatial resolution into the experiment would permit details of domain composition in monolayers to be elucidated, with the caveat that IR spatial resolution is limited to a few microns at best. The general feasibility of the approach was shown in 2006 by Steiner et al.[58]. Monolayers of octadecanephosphonic acid (OPA) attached to a microstructured aluminum oxide/gold patterned surface were formed. PM-IRRAS images were generated with a point-by-point sampling approach in a standard IR spectrometer. In these experiments, there is a trade-off between lateral spatial resolution and high sensitivity determined by the angle of incidence. Lateral resolution of ~ 15 microns produced an IR map of a strong P=O band between regions where P=O was present (aluminum oxide surface) versus regions where it was absent (gold surface). However, the maps were of marginal contrast. Changes in the optical set-up tended to degrade the spatial resolution to 45-85 microns but enhanced the sensitivity to produce better quality spectra and images.

To acquire spatially resolved IRRAS data from Langmuir films, the experiment has to be sufficiently rapid so that molecular diffusion during data collection doesn't blur the images. Increasing the brightness of a light source might help the acquisition of IRRAS data from solid substrates, but might also cause heating and convection in Langmuir films. Improvement may be possible through the use of tunable IR diode lasers and a rastering approach. In addition, incorporation of an (extremely sensitive) IR array detector might significantly decrease data acquisition times.

Finally, a novel experiment developed by Rabolt and Chase and their collaborators may provide the desired solution to rapid acquisition of IRRAS spectra as well as imaging[59,60]. They have developed a planar array infrared reflection spectrograph (PA-IRRS) in which an infrared spectrograph disperses a mid-IR spectrum onto a mercury cadmium telluride array detector. PA-IR instruments offer many advantages over conventional FT-IR instruments, including a simple experimental setup, a multichannel detection advantage, and no moving parts. In a recent report[60], the authors describe a design which can record sample and reference channels simultaneously, thereby providing good compensation of the water vapor in a IRRAS measurement. The performance of the device is shown in Figure 17, where the authors present a spectrum featuring the C=O mode of poly-L-lactic acid. The total acquisition time for 1000 frames was in 10.8 sec, while the total integration time required was 1.5 sec. The next step would be to couple the PA-IRRS device to an IR microscope.

In summary, the ability of IRRAS and PM-IRRAS to provide molecular structure and orientation information from Langmuir films is a well-proven technique in monolayer biophysics. Experimentally, the initial problems with spectral interference due to water vapor have been overcome so that spectra may be readily acquired from the Amide I spectral region, while the theoretical analysis of the band intensities appears to be robust. These considerations portend well for future applications.

Acknowledgments

Some experiments conducted at Rutgers University reported in this article were supported by NIH AI-83222. We also thank the authors of various figures (as noted) for their kindness in allowing us to reprint their work and in many cases supplying high quality figures.

References

[1]. Schürch S, Green FHY, Bachofen H. Formation and structure of surface films: captive bubble surfactometry. Biochim. Biophys. Acta 1998;1408:180–202. [PubMed: 9813315]

[2]. Clements JA. Functions of the alveolar lining. Am. Rev. Respir. Dis 1977;115:67–71. [PubMed: 577382]

[3]. Lichtenberg D, Romero G, Menashe M, Biltonen RL. Hydrolysis of dipalmitoylphosphatidylcholine large unilamellar vesicles by porcine pancreatic phospholipase A_2. J. Biol. Chem 1986;261:5334–5340. [PubMed: 3754258]

[4]. Möhwald H. Direct characterization of monolayers at the air-water interface. Thin Solid Films 1988;159:1–15.

[5]. Möhwald H. Phospholipid and phospholipid-protein monolayers at the air/water interface. Annu. Rev. Phys. Chem 1990;41:441–476. [PubMed: 2257038]

[6]. McConnell HM. Structures and transitions in lipid monolayers at the air-water interface. Annu. Rev. Phys. Chem 1991;42:171–195.

[7]. Hönig D, Möbius D. Direct visualization of monolayers at the air-water interface by Brewster angle microscopy. J. Phys. Chem 1991;95:4590–4592.

[8]. Dluhy RA, Cornell DG. In situ measurement of the infrared spectra of insoluble monolayers at the air-water interface. J. Phys. Chem 1985;89:3195–3197.

[9]. Dluhy RA. Quantitative external reflection infrared spectroscopic analysis of insoluble monolayers spread at the air-water interface. J. Phys. Chem 1986;90:1373–1379.

[10]. Dluhy RA, Wright NA, Griffiths PR. In situ measurement of the FT-IR spectra of phospholipid monolayers at the air/water interface. Appl. Spectrosc 1988;42:138–141.

[11]. Dluhy RA, Mitchell ML, Pettenski T, Beers J. Design and interfacing of an automated Langmuir-type film balance to an FT-IR spectrometer. Appl. Spectrosc 1988;42:1289–1293.

[12]. Flach CR, Brauner JW, Mendelsohn R. Calcium ion interactions with insoluble phospholipid monolayer films at the A/W interface. External reflection-absorption studies. Biophys. J 1993;65:1994–2001. [PubMed: 8298029]

[13]. Gericke A, Flach CR, Mendelsohn R. Structure and orientation of lung surfactant SP-C and L-α-dipalmitoylphosphatidylcholine in aqueous monolayers. Biophys. J 1997;73:492–499. [PubMed: 9199811]

[14]. Blaudez D, Buffeteau T, Cornut JC, Desbat B, Escafre N, Pezolet M, Turlet JM. Polarization-modulated FT-IR spectroscopy of a spread monolayer at the air/water interface. Appl. Spectrosc 1993;47:869–874.

[15]. Cornut I, Desbat B, Turlet JM, Dufourcq J. In situ study by polarization modulated Fourier transform infrared spectroscopy of the structure and orientation of lipids and amphipathic peptides at the air-water interface. Biophys. J 1996;70:305–312. [PubMed: 8770206]

[16]. Ulrich W-P, Vogel H. Polarization-modulated FTIR spectroscopy of lipid/gramicidin monolayers at the air/water interface. Biophys. J 1999;76:1639–1647. [PubMed: 10049344]

[17]. Kerth A, Erbe A, Dathe M, Blume A. Infrared reflection absorption spectroscopy of amphipathic model peptides at the air/water interface. Biophys. J 2004;86:3750–3758. [PubMed: 15189871]

[18]. Dluhy RA, Stephens SM, Widayati S, Williams AD. Vibrational spectroscopy of biophysical monolayers. Applications of IR and Raman spectroscopy to biomembrane model systems at interfaces. Spectrochimica Acta Part A 1995;51:1413–1447.

[19]. Dluhy RA. Infrared spectroscopy of biophysical monolayer films at interfaces. Theory and applications. Appl. Spectrosc. Reviews 2000;35:315–351.

[20]. Blaudez D, Buffeteau T, Desbat B, Turlet JM. Infrared and Raman spectroscopies of monolayers at the air-water interface. Current Opinion in Colloid & Interface Science 1999;4:265–272.

[21]. Mendelsohn R, Brauner JW, Gericke A. External Infrared Reflection Absorption Spectrometry of Monolayer Films At the Air-Water Interface. Annu. Rev. Phys. Chem 1995;46:305–334.

[22]. Mendelsohn, R.; Flach, CR. Handbook of Vibrational Spectroscopy. Chalmers, JM.; Griffiths, PR., editors. Vol. vol. 2. John Wiley and Sons, Ltd.; Chichester, UK: 2002. p. 1028-1041.

[23]. Flach CR, Brauner JW, Taylor JW, Baldwin RC, Mendelsohn R. External reflection FTIR of peptide monolayer films *in situ* at the air/water interface - experimental design, spectra-structure correlations, and effects of hydrogen-deuterium exchange. Biophys. J 1994;67:402–410. [PubMed: 7919013]

[24]. Blaudez D, Turlet JM, Dufourcq J, Bard D, Buffeteau T, Desbat B. Investigations at the air/water interface using polarization modulation IR spectroscopy. J.Chem.Soc.,Faraday Trans 1996;92:525–530.

[25]. Snyder RG, Schachtschneider JH. Vibrational analysis of the n-paraffins-I. Assignments of infrared bands in the spectra of C_3H_8 through $C_{19}H_{40}$, Spectrochim. Acta 1963;19:85–116.

[26]. Snyder RG. Vibrational correlation splitting and chain packing for the crystalline n-alkanes. J. Chem. Phys 1979;71:3229–3235.

[27]. Zerbi G, Magni R, Gussoni M, Moritz K. Holland, Bigotto AB, Dirlikov S. Molecular mechanics for phase transition and melting of *n*-alkanes: a spectroscopic study of molecular mobility of solid *n*-nonadecane. J. Chem. Phys 1981;75:3175–3194.

[28]. Simanouti T, Mizushima S-I. The constant frequency Raman lines of n-paraffins. J. Chem. Phys 1949;17:1102–1106.

[29]. Tasumi M, Shimanouchi T. Crystal vibrations and intermolecular forces of polymethylene crystals. J. Chem. Phys 1965;43:1245–1258.

[30]. Brauner JW, Dugan C, Mendelsohn R. ^{13}C isotope labeling of hydrophobic peptides. Origin of the anomalous intensity distribution in the infrared Amide I spectral region of β-sheet structures. J. Am. Chem. Soc 2000;122:677–683.

[31]. Bryan MA, Brauner JW, Anderle G, Flach CR, Brodsky B, Mendelsohn R. FTIR studies of collagen model peptides: Complementary experimental and simulation approaches to conformation and unfolding. J. Am. Chem. Soc 2007;129:7877–7884. [PubMed: 17550251]

[32]. Brauner JW, Flach CR, Mendelsohn R. A quantitative reconstruction of the Amide I contour in the IR spectra of globular proteins: From structure to spectrum. J. Am. Chem. Soc 2005;127:100–109. [PubMed: 15631459]

[33]. Kuzmin VL, Michailov AV. Molecular theory of light reflection and applicability limits of the macroscopic approach. Opt. Spectrosc. (USSR) 1981;51:383–385.

[34]. Kuzmin VL, Romanov VP, Michailov AV. Reflection of light at the boundary of liquid systems and structure of the surface layer: A review. Opt. Spectrosc 1992;73:1–26.

[35]. Gericke A, Michailov AV, Hühnerfuss H. Polarized external infrared reflection-absorption spectrometry at the air/water interface: comparison of experimental and theoretical results for different angles of incidence. Vibrational Spectroscopy 1993;4:335–348.

[36]. Flach CR, Xu Z, Bi X, Brauner JW, Mendelsohn R. Improved IRRAS apparatus for studies of aqueous monolayer films: Determination of the orientation of each chain in a fatty-acid homologous Ceramide 2. Appl. Spectrosc 2001;55:1060–1066.

[37]. Brauner JW, Flach CR, Xu Z, Bi X, Lewis RNAH, McElhaney RN, Gericke A, Mendelsohn R. Quantitative functional group orientation in Langmuir films by infrared reflection-absorption spectroscopy: C=O groups on behenic acid methyl ester and *sn*2-^{13}C-DSPC. J. Phys. Chem. B 2003;107:7202–7211.

[38]. Flach CR, Gericke A, Mendelsohn R. Quantitative determination of molecular chain tilt angles in monolayer films at the air/water interface - infrared reflection/absorption spectroscopy of behenic acid methyl ester. J. Phys. Chem. B 1997;101:58–65.

[39]. Pelletier I, Bourque H, Buffeteau T, Blaudez D, Desbat B, Pézolet M. Study by infrared spectroscopy of ultrathin films of behenic acid methyl ester on solid substrates and at the air/water interface. J. Phys. Chem. B 2002;106:1968–1976.

[40]. Hunt RD, Mitchell ML, Dluhy RA. The interfacial structure of phospholipid monolayer films: an infrared reflectance study. Journal of Molecular Structure 1989;214:93–109.

[41]. Saccani J, Castano S, Beaurain F, Laguerre M, Desbat B. Stabilization of phospholipid multilayers at the air-water interface by compression beyond the collapse: A BAM, PM-IRRAS, and molecular dynamics study. Langmuir 2004;20:9190–9197. [PubMed: 15461505]

[42]. Lad MD, Birembaut F, Frazier RA, Green RJ. Protein-lipid interactions at the air/water interface. Phys. Chem. Chem. Phys 2005;7:3478–3485. [PubMed: 16273149]

[43]. Flach CR, Cai P, Dieudonné D, Brauner JW, Keough KMW, Stewart J, Mendelsohn R. Location of structural transitions in an isotopically labeled lung surfactant SP-B peptide by IRRAS. Biophys. J 2003;85:340–349. [PubMed: 12829488]

[44]. Dyck M, Kerth A, Blume A, Losche M. Interaction of the neurotransmitter, Neuropeptide Y, with phopholipid membranes: Infrared spectroscopic characterization at the air/water interface. J. Phys. Chem. B 2006;110:22152–22159. [PubMed: 17078651]

[45]. Monks SA, Karagianis G, Howlett GJ, Norton RS. Solution structure of human neuropeptide Y. J. Biomol. NMR 1996;8:379–390. [PubMed: 9008359]

[46]. Bi X, Taneva S, Keough KMW, Mendelsohn R, Flach CR. Thermal stability and DPPC/Ca^{2+} interactions of pulmonary surfactant SP-A from bulk phase and monolayer IR spectroscopy. Biochemistry 2001;40:13659–13669. [PubMed: 11695915]

[47]. Nag K, Perezgil J, Cruz A, Keough KMW. Fluorescently Labeled Pulmonary Surfactant Protein C in Spread Phospholipid Monolayers. Biophys. J 1996;71:246–256. [PubMed: 8804608]

[48]. Estrela-Lopis I, Brezesinski G, Mohwald H. Dipalmitoyl-phosphatidylcholine/phospholipase D interactions investigated with polarization-modulated infrared reflection absorption spectroscopy. Biophys. J 2001;80:749–754. [PubMed: 11159442]

[49]. Wang X, Zheng S, He Q, Brezesinski G, Mohwald H, Li J. Hydrolysis reaction analysis of L-α-distearoylphosphatidylcholine monolayer catalyzed by phospholipase A_2 with polarization-modulation infrared reflection absorption spectroscopy. Langmuir 2005;21:1051–1054. [PubMed: 15667188]

[50]. Wagner K, Desbat B, Brezesinski G. Liquid-liquid immiscibility in model membranes activates secretory phopholipase A_2. Biochim.Biophys.Acta 2008;1778:166–174. [PubMed: 17964533]

[51]. Wang L, Brauner JW, Mao G, Crouch E, Seaton B, Head J, Smith K, Flach CR, Mendelsohn R. Interaction of recombinant surfactant protein D with lipopolysaccharide: Conformation and orientation of bound protein by IRRAS and simulations. Biochemistry 2008;47:8103–8113. [PubMed: 18620419]

[52]. Wang L, Cai P, Galla H-J, He H, Flach CR, Mendelsohn R. Monolayer–multilayer transitions in a lung surfactant model: IR reflection–absorption spectroscopy and atomic force microscopy. Eur. Biophys. J 2005;34:243–254. [PubMed: 15645307]

[53]. Brockman JM, Wang Z, Notter RH, Dluhy R. Effect of hydrophobic surfactant proteins SP-B and SP-C on binary phospholipid monolayers II. Infrared external reflectance-absorption spectroscopy. Biophys. J 2003;84:326–340. [PubMed: 12524286]

[54]. Nakahara H, Dudek A, Nakamura Y, Lee S, Chang CH, Shibata O. Hysteresis behavior of amphiphilic model peptide in lung lipid monolayers at the air-water interface by an IRRAS measurement. Colloid Surf. B-Biointerfaces 2009;68:61–67.

[55]. Wang H, Head J, Kosma P, Brade H, Muller-Loennies S, Sheikh S, McDonald B, Smith K, Cafarella T, Seaton B, Crouch E. Recognition of Heptoses and the Inner Core of Bacterial Lipopolysaccharides by Surfactant Protein D. Biochemistry 2008;47:710–720. [PubMed: 18092821]

[56]. Hakansson S, Lim NK, Hoppe H-J, Reid KBM. Crystal structure of the trimeric α-helical coiled-coil and the three lectin domains of human lung surfactant protein D. Structure 1999;7:255–264. [PubMed: 10368295]

[57]. Shrive AK, Tharia HA, Strong P, Kishore U, Burns I, Rizkallah PJ, Reid KBM, Greenhough TJ. High-resolution structural insights into ligand binding and immune cell recognition by human lung surfactant protein D. J. Mol. Biol 2003;331:509–523. [PubMed: 12888356]

[58]. Steiner G, Sablinskras V, Kitsche M, Salzer R. Polarization modulation-infrared reflection absorption spectroscopic mapping. Anal. Chem 2006;78:2487–2493. [PubMed: 16615754]

[59]. Pellerin C, Snively CM, Chase DB, Rabolt JF. Performance and application of a new planar array infrared spectrograph operating in the mid-infrared (2000-975 cm^{-1}) fingerprint region. Appl. Spectrosc 2004;58:639–646. [PubMed: 15198813]

[60]. Kim YS, Snively CM, Rabolt JF, Chase B. Development of a planar array infrared reflection spectrograph for reflection-absorption spectroscopy of thin films at metal and water surfaces. Appl. Spectrosc 2007;61:916–920. [PubMed: 17910786]

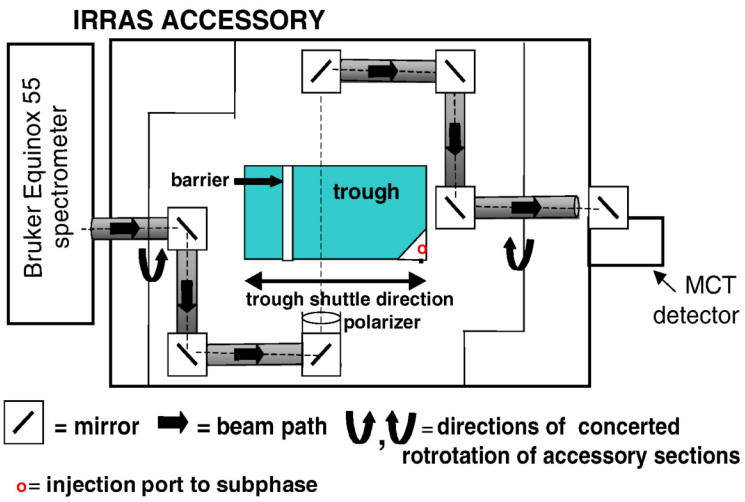

Figure 1.

IRRAS accessory currently in use at Rutgers University. The Wilhemy plate is placed on the right hand side of the trough. The reference channel is to the left of the barrier. The entire trough shuttles as indicated to sample the desired channel. The incident light is guided to the surface via three mirrors. The beam path is represented as a dashed line. The reflected light follows an equivalent optical path. The angles of incidence and reflection as well as the state of polarization are under computer control. (reprinted with permission (pending) from ——————).

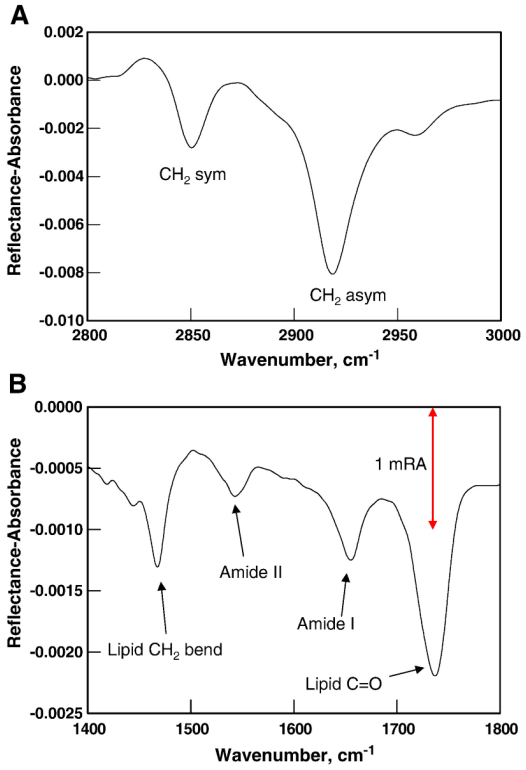

Figure 2.

IRRAS spectrum of the 4 component system DPPC/DPPG/cholesterol/SP-C on a D_2O subphase demonstrating the highS/N ratio achieved with current instrumentation in A) the methylene stretching region, 2800-3000 cm^{-1} and B) the 1400-1800 cm^{-1} region containing vibrations from the lipid and protein constituents as marked.

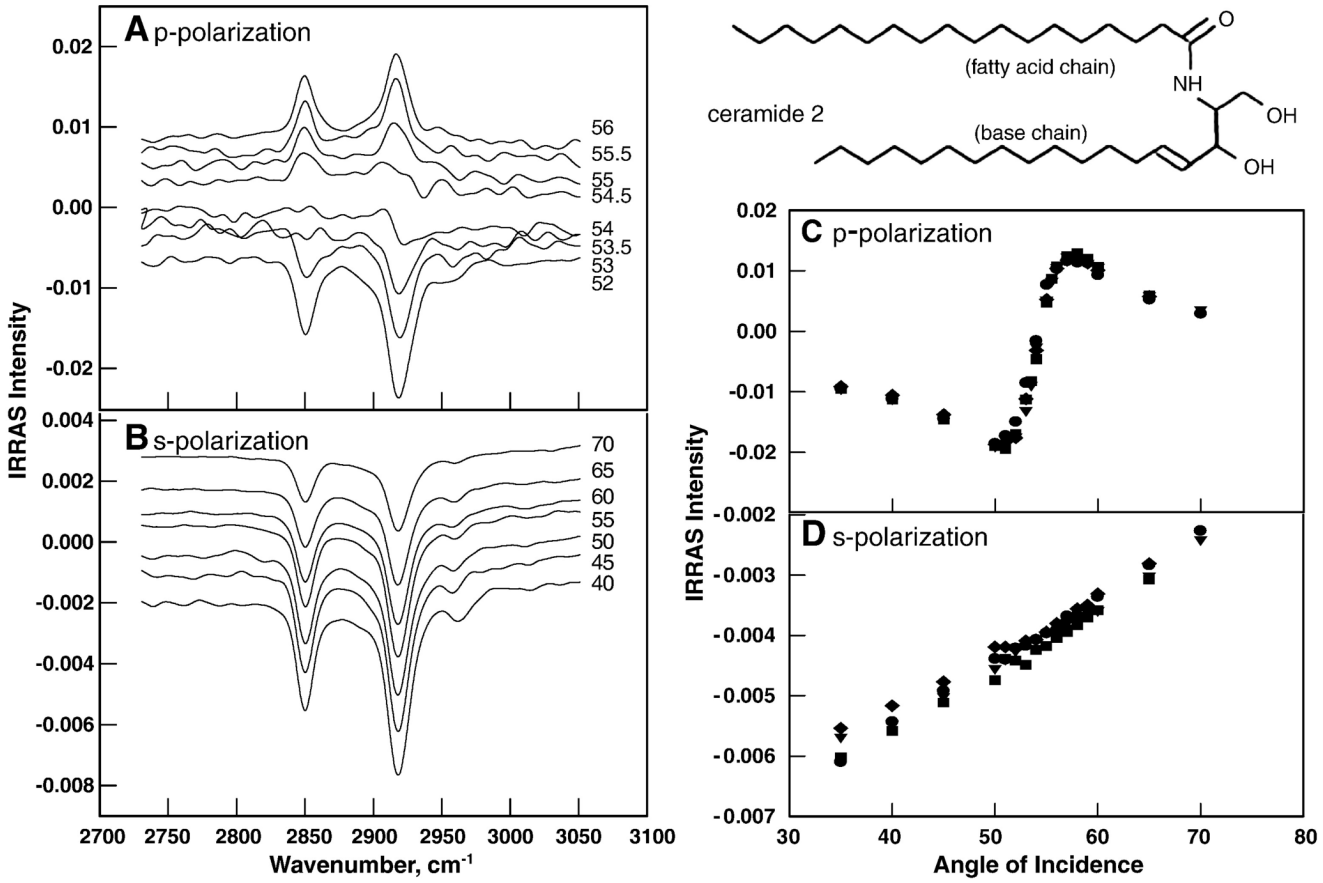

Figure 3.

Precision and accuracy in quantitative IRRAS measurements. The molecule studied is a synthetic ceramide lipid model, whose structure is illustrated. A) Spectra of the CH_2 stretching region acquired with p-polarized radiation over a fairly narrow range of incident angles. Note the sign change of the RA at the Brewster angle. Further details in the text. B) Spectra of the CH_2 stretching region acquired with s-polarized radiation over a range of incident angles. C) Reproducibility of the p-polarized intensity of the CH_2 asymmetric stretch (2920 cm^{-1}) as a function of angle of incidence. Data for 4 independent films are overlaid. D) Reproducibility of the s-polarized intensity for the same band as a function of angle of incidence. (reprinted with permission (pending) from ——————).

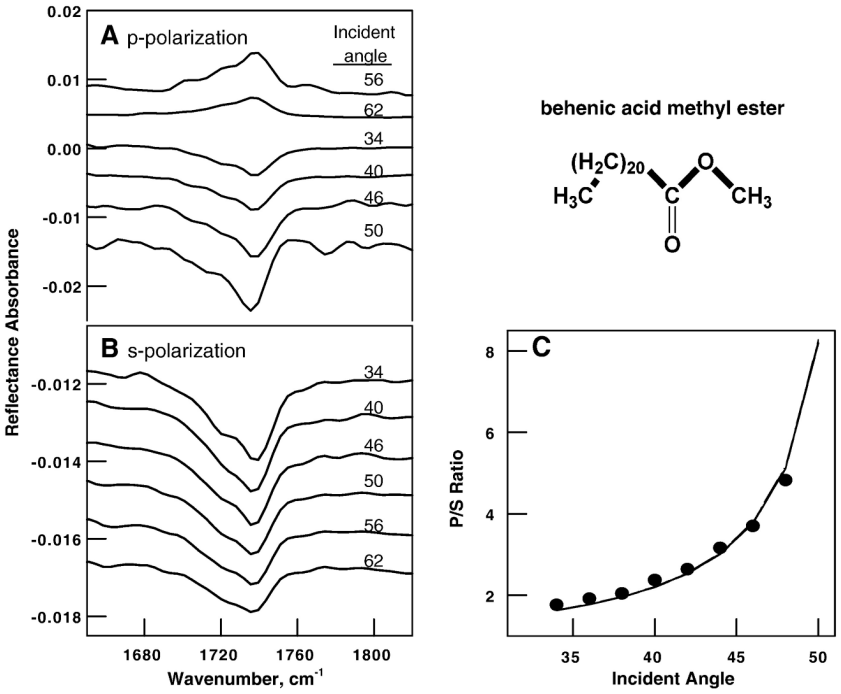

Figure 4.

Demonstration of the validity of the theoretical formalism used to calculate tilt angles of functional groups. The molecule is behenic acid methyl ester (structure shown). IRRAS spectral data (D_2O subphase) for p-polarized and s-polarized radiation are shown in A) and B), respectively. The complex C=O contour was resolved and the orientation of the 1737 cm^{-1} band arising from unhydrated C=O groups was determined. The experimental p/s band intensity ratios are shown as a function of angle of incidence in C) along with the theoretical simulations for a 90° tilt angle. (reprinted with permission (pending) from ————————).

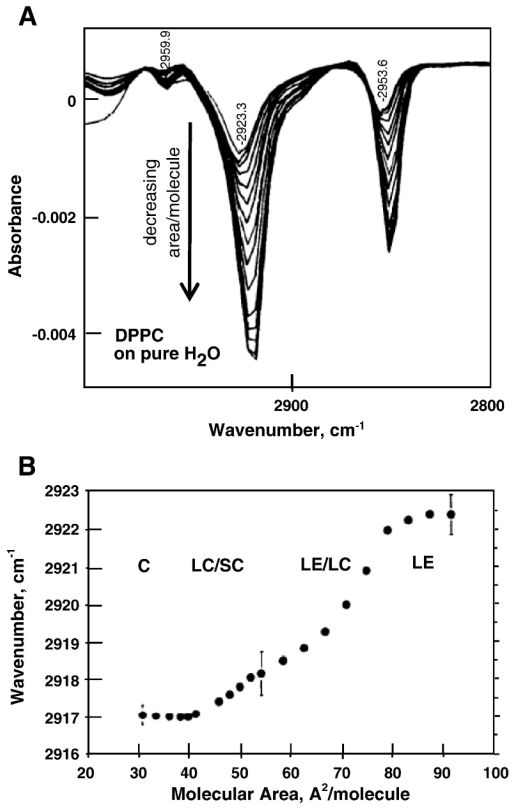

Figure 5.

The first IRRAS determination of the determination of chain order for various phases of a lipid (DPPC) film. A) IRRAS spectra of DPPC monolayers at decreasing molecular areas as shown by the direction of the arrow B) The frequency of the asymmetric CH_2 stretching vibration plotted as a function of molecular area for the various DPPC phases as indicated. (reprinted with permission (pending) from ———————— and from Professor Rich Dluhy, University of Georgia).

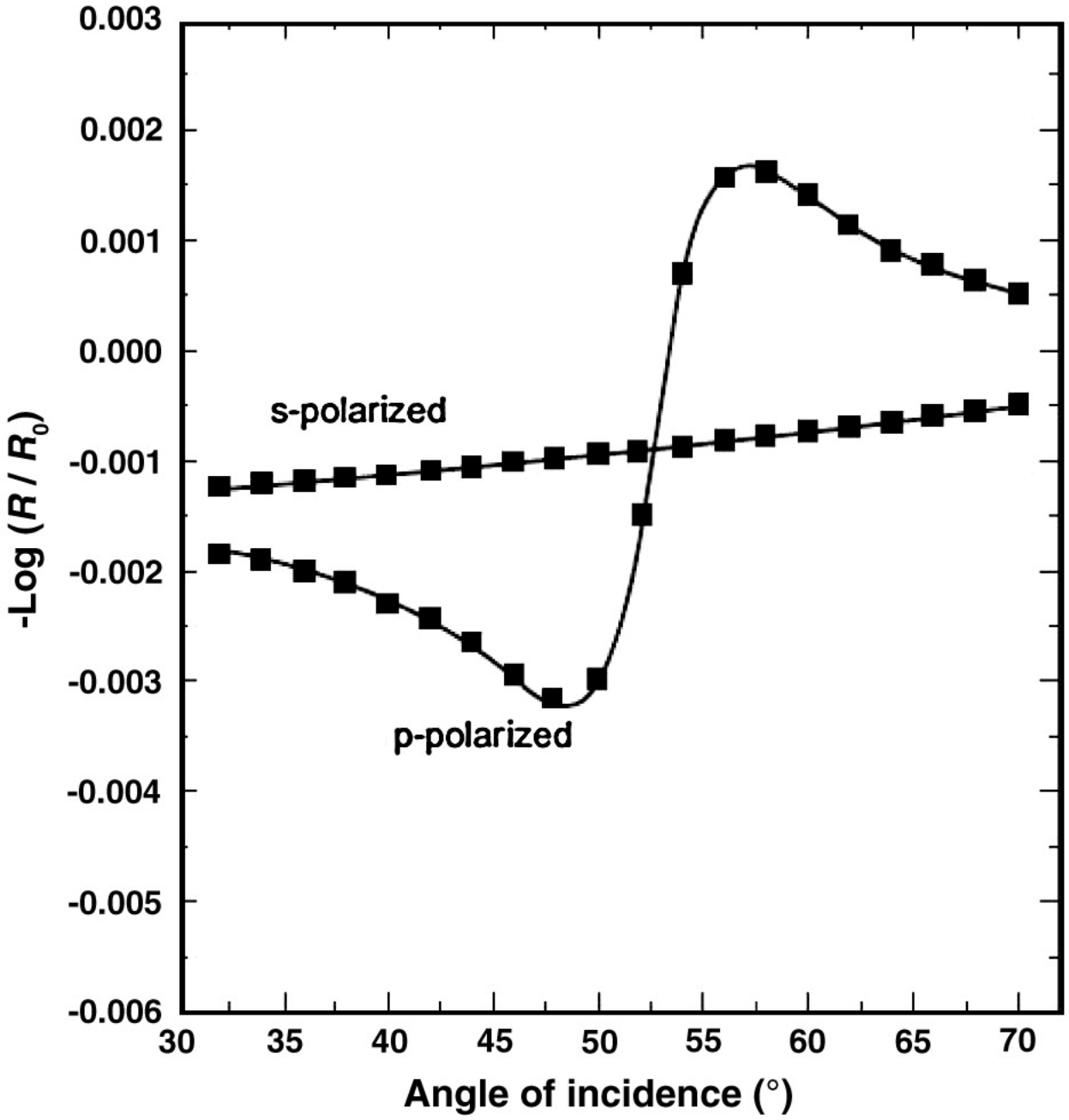

Figure 6.

Measured (■) and calculated (–) RA vs angle of incidence for the symmetric CD_2 stretching vibration of a monolayer of DPPC-d_{62} on an H_2O subphase at 21°C and a surface pressure of 28mN/m. The best fit to the data was found using an acyl chain tilt angle of 26°. The calculated lines are shown along with the experimental data for s- and p-polarized light. (reprinted with permission (pending) from ——————). (Figure courtesy of Professor Arne Gericke, of Kent State University).

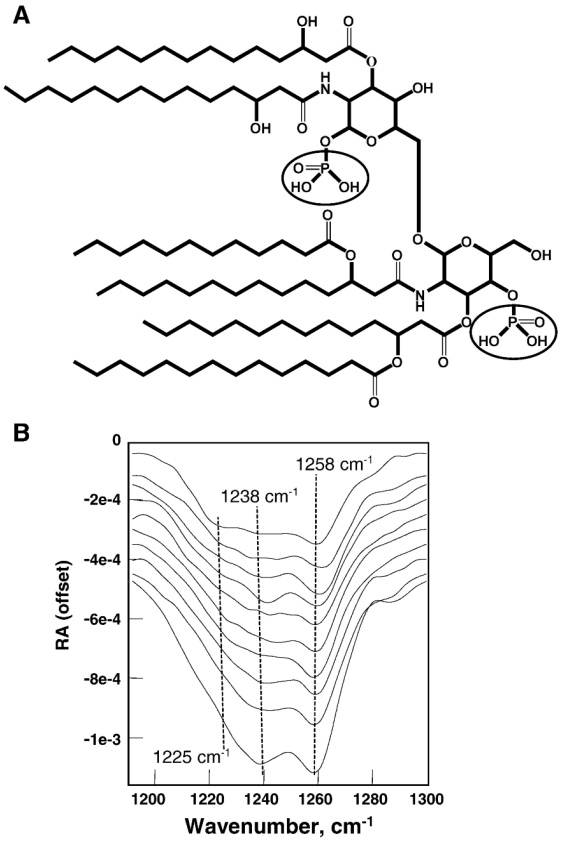

Figure 7.

Sensitivity of the phosphate vibrations to hydration. A) Structure of Lipid A. B) S-polarized IRRAS spectra as a function of surface pressure, which increases from the top to the bottom spectrum. Spectra are offset for clarity. The phosphate vibrations at 1258, 1238 and 1225 cm^{-1} represent unhydrated, monohydrated and dihydrated forms of particular phosphates in the molecule.

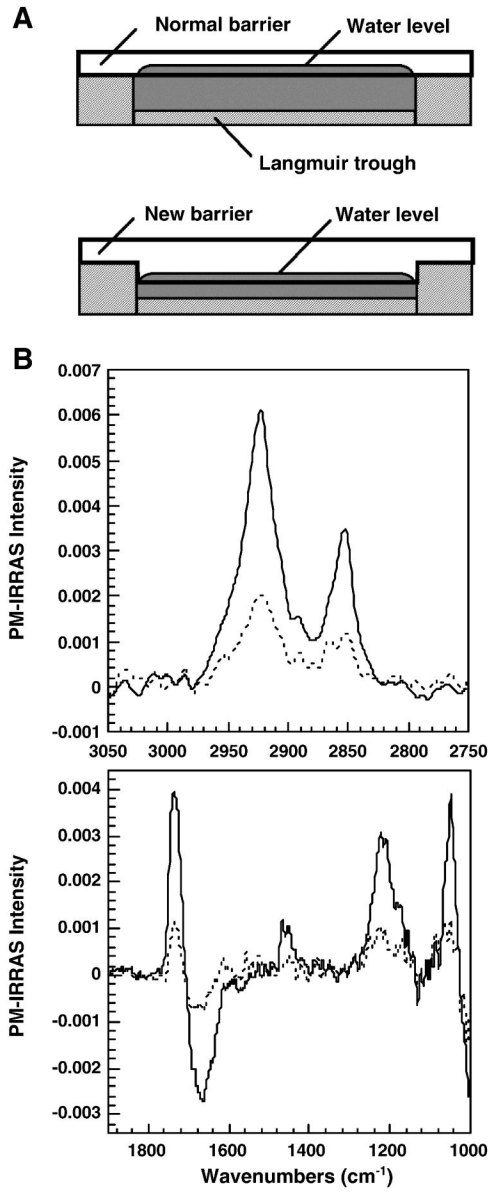

Figure 8.

Langmuir trough design for examination of multilayer states of aqueous films: A) top, normal barrier design; bottom, embedded barrier design permitting acquisition of IRRAS spectra at high surface pressures. B) PM-IRRAS spectra of a DOPS monolayer at 26 mN/m (dashed line) and of a trilayer (solid line) at 44 mN/m in the alkyl chain methylene stretching region (top panel in B) and in the polar headgroup vibration range (bottom panel in B). (reprinted with permission (pending) from ——————— (Figure courtesy of Professor Bernard Desbat, CNRS, Talence Cedex, France).

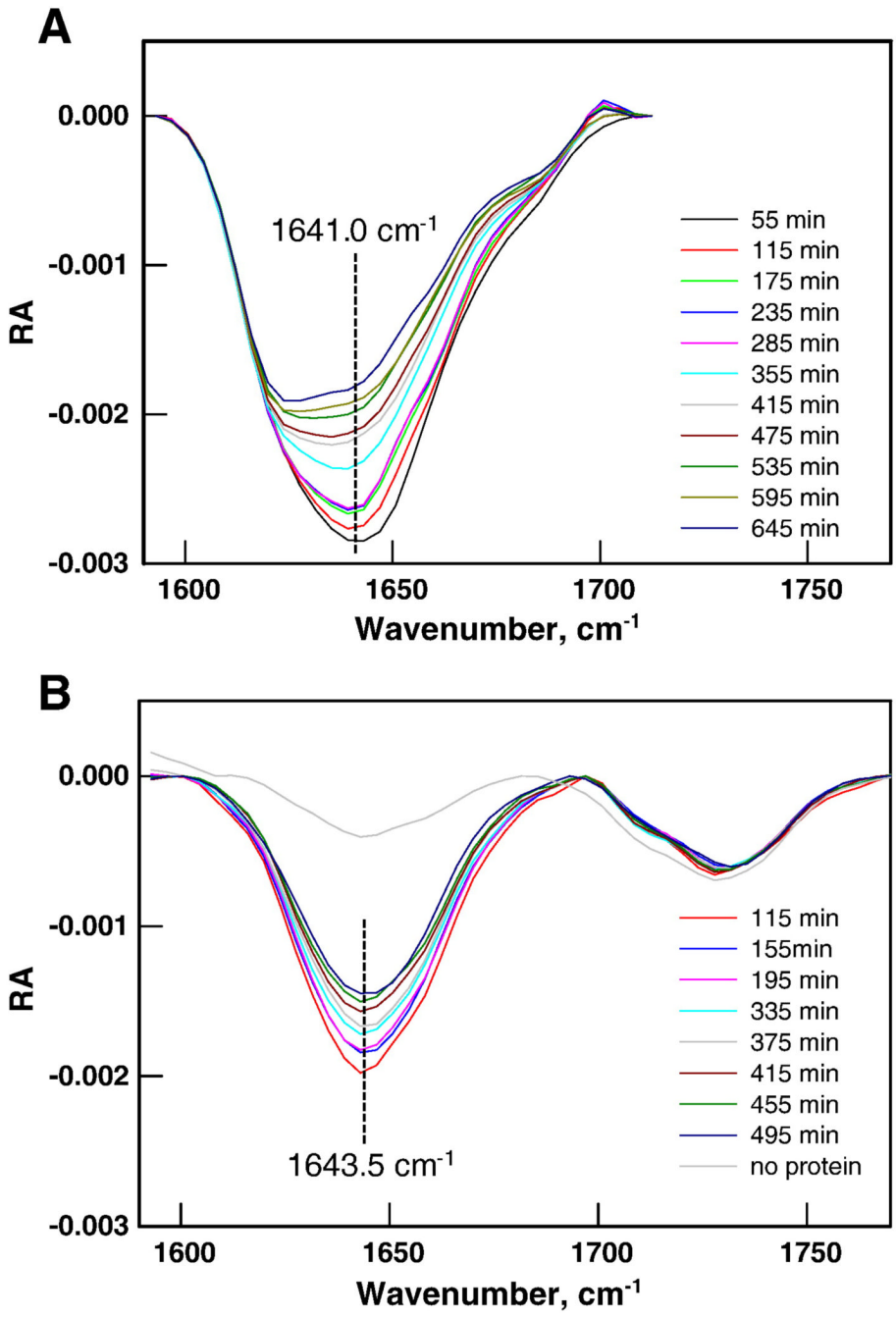

Figure 9.

Temporal stability of pulmonary surfactant SP-A NCRD Langmuir films in the absence (A) and presence (B) of a lipid A film at a surface pressure of 25 mN/m on a D_2O Ca^{2+}-containing buffer.

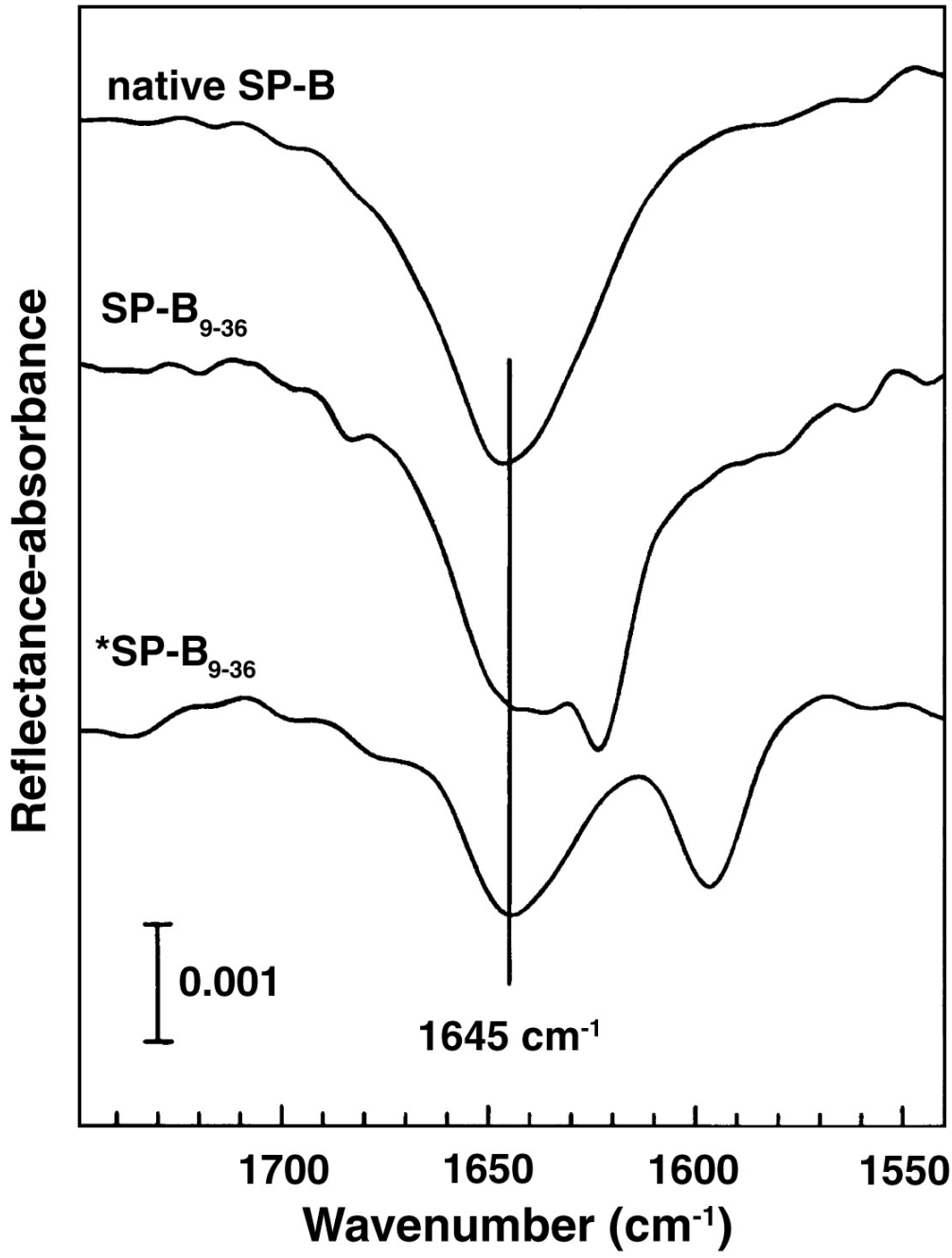

Figure 10.

Isotope labeling delineates the β-sheet region in the synthetic fragment NH_2-WLARALIKRIAQMIPKGA*LA*VA*VA*Q-VCR-COOH of pulmonary surfactant SP-B. Top spectrum, native SP-B; middle spectrum, unlabeled synthetic peptide sequence; bottom spectrum, peptide with alanines labeled (*following labeled residues). (reprinted with permission (pending) from ————————).

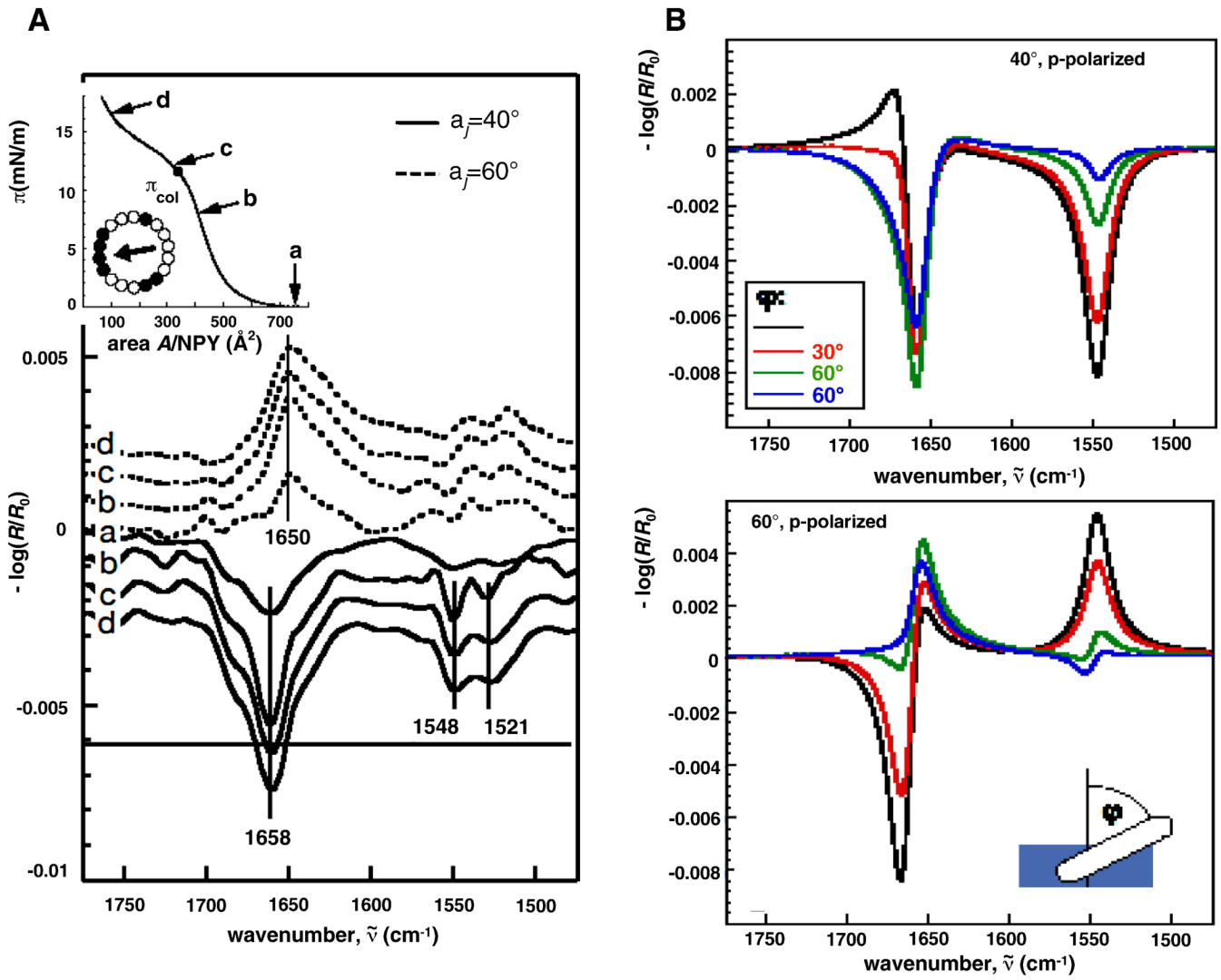

Figure 11.

Determination of the orientation of Neuropeptide Y in a Langmuir film during compression. Characters adjacent to the p-polarized spectra in A), bottom panel correspond to pressures in the π-A isotherm shown in the inset (top left) as follows (a: π =0; b: 8mN/m; c:12 mN/m; d: 16 mN/m). Spectra were acquired for angles of incidence of 40° (solid line) and 60°, (dashed line). Also shown is a helical wheel representation of the peptide α-helix (black: hydrophobic residues; white hydrophilic residues; arrow: direction of the hydrophobic moment). B) Simulations of the Amide I and II bands (p-polarization for angles of incidence of 40° (top) and 60°(bottom) of neuropeptide Y for different tilt angles, φ (defined in the bottom panel), of the α-helix from the surface normal. (reprinted with permission (pending) from ————————) (Figure courtesy of Professor Mathias Lösche, Carnegie-Mellon University).

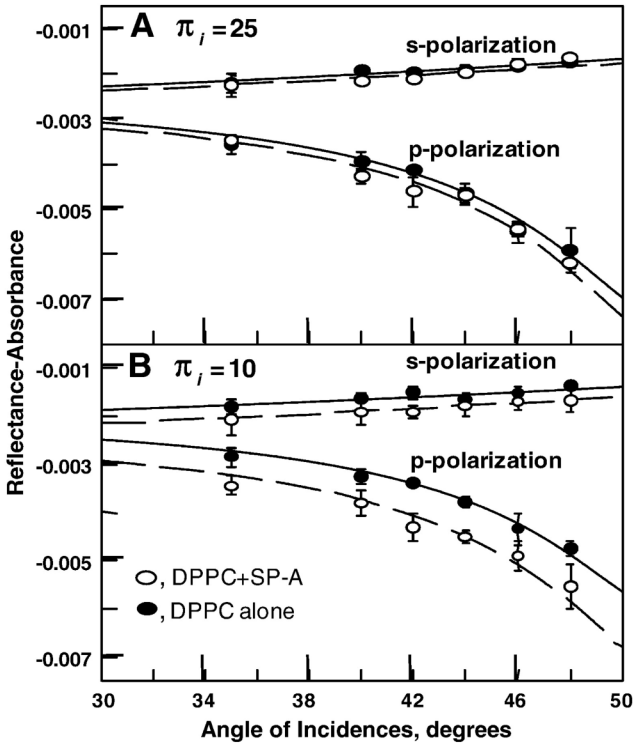

Figure 12.

Pulmonary surfcatant SP-A-induced changes in the tilt angle of the DPPC acyl chains at two surface pressures and polarizations: A) π =25 mN/m, B) π =10 mN/m. DPPC films (o), DPPC/SP-A films (•), calculated curves A) pure DPPC (solid line) chain tilt angle= 32°; DPPC/SP-A (dashed line) chain tilt angle =31° B) pure DPPC (solid line) chain tilt angle= 35°; DPPC/SP-A (dashed line) chain tilt angle =28° (reprinted with permission (pending) from ————————).

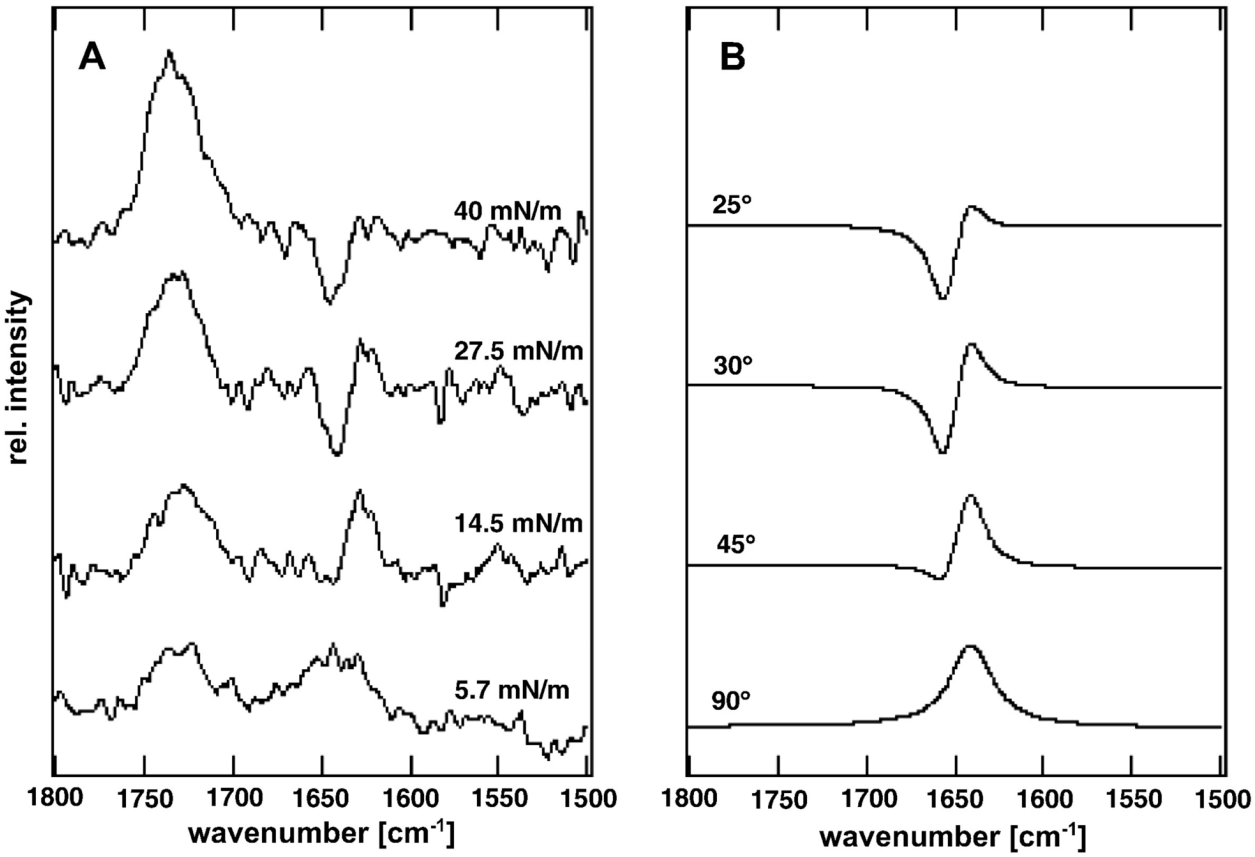

Figure 13.

A) PM-IRRAS spectra of a DMPC/gramicidin A layer (8:1 molar ratio) at the indicated film pressures on a D_2O subphase. B) Simulated PM-IRRAS spectra of the amide I band of gramicidin A at the indicated tilt angles on a D_2O subphase. (reprinted with permission (pending) from ——————) (Figure courtesy of Professor Horst Vogel, Ecole Polytechnique Federale de Lausanne and Dr. Peter Ulrich, SCIPROM, St-Sulpice, Switzerland).

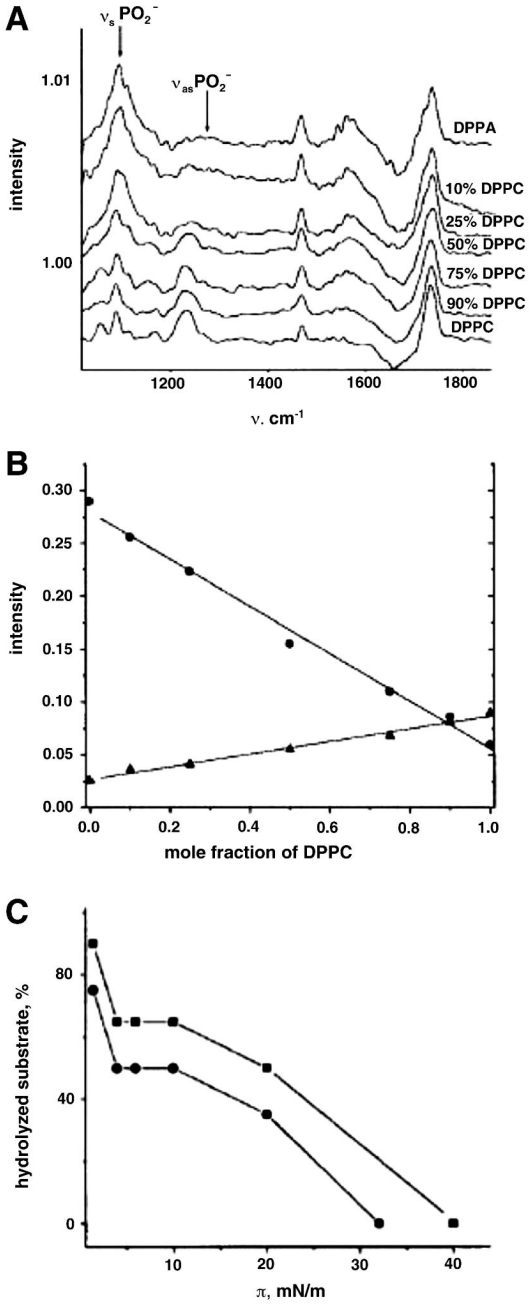

Figure 14.

Phospholipid interactions with Phospholipase D. A) PM-IRRAS spectra of different DPPC/DPPA mixtures at π = 40 mN/m. B) Integrated intensity of the phosphate vibrations as a function of the DPPC mole fractions in mixtures with DPPA. (•) sum of the symmetric PO_2^- and CO(P) modes, (▲) antisymmetric PO_2^- vibration band. C) hydrolysis yield catalyzed by 25 (•) and 255 (■) units of Phospholipase D. (reprinted with permission (pending) from ——— and Professor Gerald Brezesinski, Max Planck Institute of Colloids and Interfaces, Golm/Potsdam, Germany).

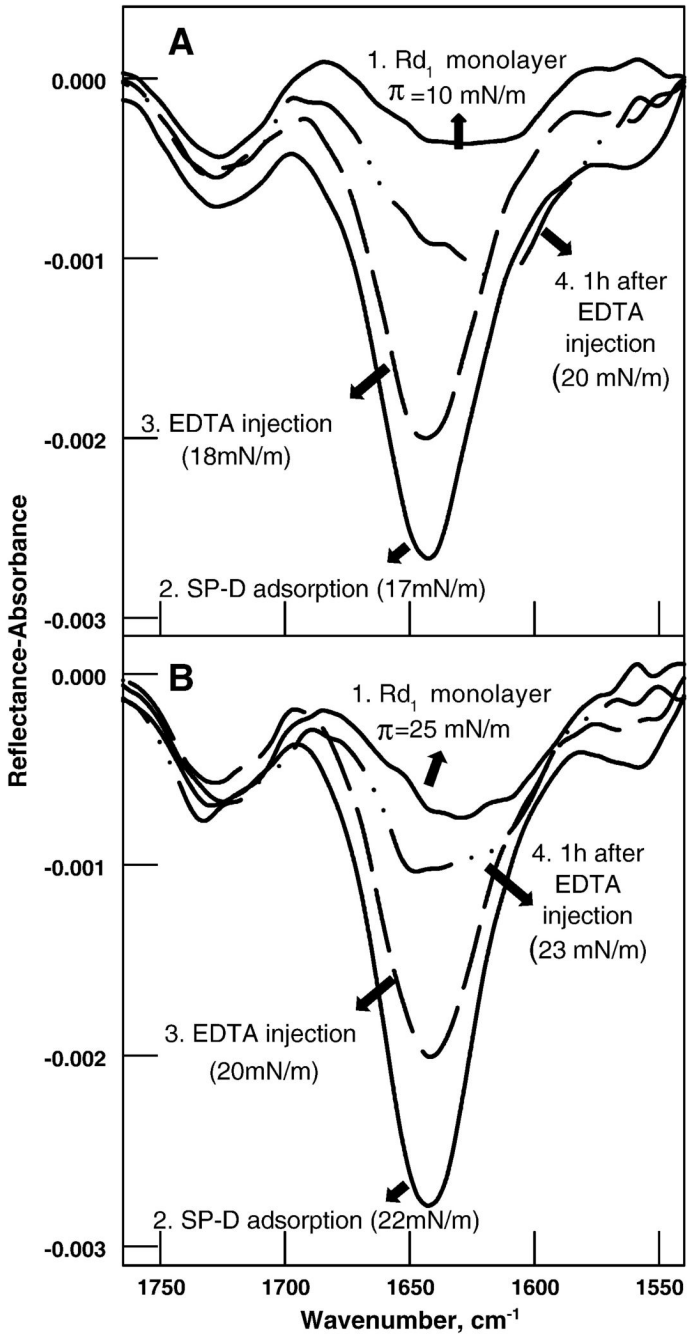

Figure 15.

IRRAS spectra (1765-1540 cm^{-1}) of human SP-D NCRD adsorption to Rd_1 LPS monolayers initially compressed to (A) π = 10 mN/m and (B) π = 25 mN/m. In each panel, the spectrum labeled: (1) was acquired prior to protein injection, (2) following protein injection under the lipid monolayer and pressure equilibration, (3) 10 min following subphase injection of an EDTA solution, and (4) 1 h after the EDTA injection. Surface pressures at the various stages are noted. The lipid C=O at ~1735 cm^{-1} remains essentially unchanged under the various conditions demonstrating the stability of the LPS monolayer. A weak, broad Amide I feature (~1620-1650 cm^{-1}) arises from LPS in (1), both panels, but is overwhelmed by the intense

Amide I band resulting from adsorbed SP-D in (2) and (3). Details of the EDTA injection are discussed in the text. (reprinted with permission (pending) from ————————).

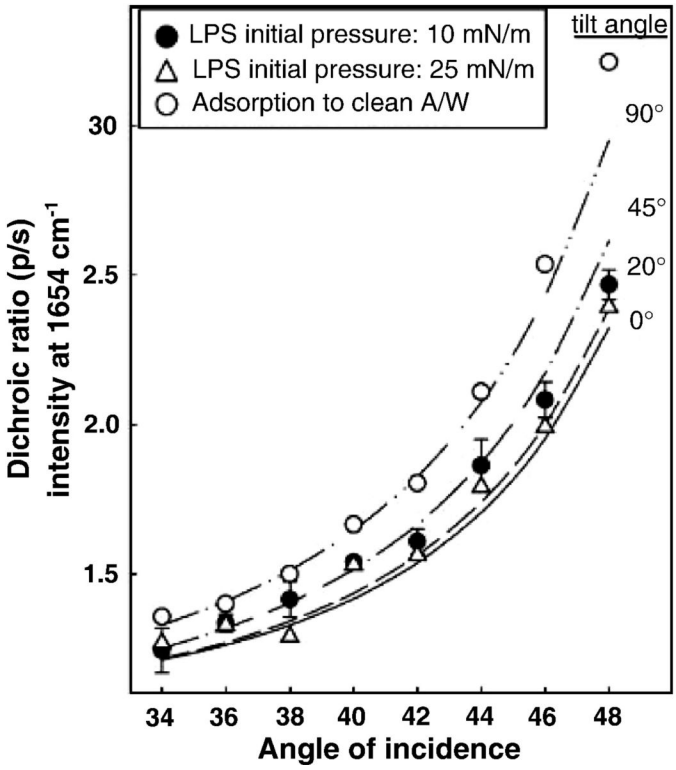

Figure 16.

Comparison of dichroic ratios of Amide I intensities at 1654 cm^{-1} as a function of angle of incidence from experimental (symbols) versus simulated (lines) data to determine the orientation of the neck region in SP-D NCRD under various conditions. Experimental values were obtained from SP-D adsorption to: (○) a clean air/water interface, (●) an LPS monolayer at Π = 10 mN/m, and (△) an LPS monolayer at Π = 25 mN/m. The mean and standard deviation for four experiments are shown for the π= 10 mN/m experiment, and averages for two experiments are shown for the two remaining datasets. Dichroic ratios are plotted from simulations conducted at particular neck axis tilt angles (0, 20 45, 90°) as marked. (reprinted with permission (pending) from ————————).

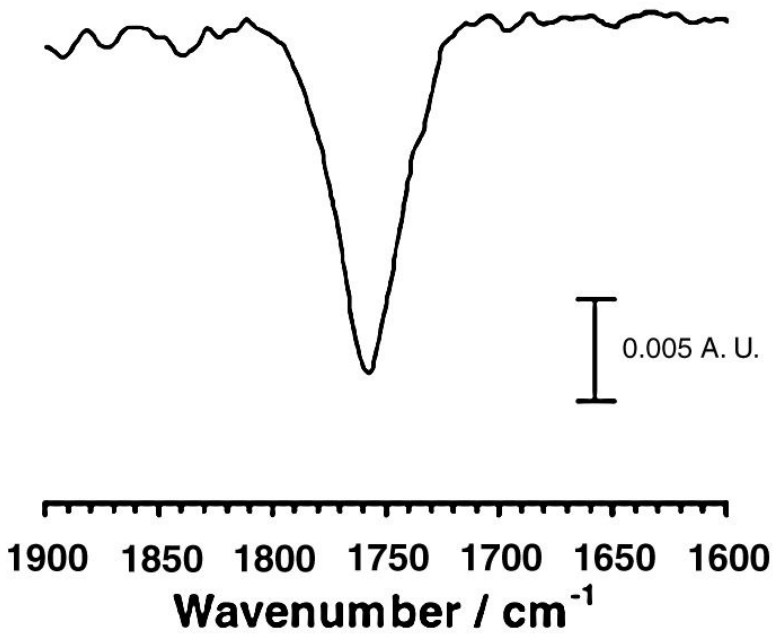

Figure 17.

Poly-L Lactic acid spectrum obtained with PA-IRRS on a water subphase at 45° angle of incidence. Total acquisition time : 10.8 s for 1000 frames; total integration time :1.5 s. (reprinted with permission (pending) from ———————— and from Professor John Rabolt, University of Delaware).

Table 1

IR modes used for analysis of IRRAS spectra

Mode	Wavenumber (cm-1)
Lipids	
Acyl chain modes	
CH_2 symmetric stretch	2849-2854
CH_2 asymmetric stretch	2916-2924
CD_2 symmetric stretch	2087-2100
CD_2 asymmetric stretch	2190-2200
CH_2 scissoring	1462, 1473 1468
CD_2 scissoring	1086, 1094 1089

Mode	Wavenumber (cm-1)
Polar region modes	
C=O stretch (ester)	1710-1740
C=O stretch (fatty acid)	1690-1740
PO_2^- asymmetric stretch	1220-1250
PO_2^- symmetric stretch	~1090
Peptide bond modes	
Amide I (mostly C=O stretch)	1610-1690
Amide II (N-H in-plane bend + C-N stretch)	1520-1560
Amide A (N-H stretch)	3200-3400